Inorg. Chem. **2007**, *46*, 607–609

Inorganic Chemistry
Communication

Ground- and Excited-State Reactivity of Iron Porphyrinogens

Julien Bachmann, Justin M. Hodgkiss, Elizabeth R. Young, and Daniel G. Nocera*

Department of Chemistry, 6-335, Massachusetts Institute of Technology, 77 Massachusetts Avenue, Cambridge, Massachusetts 02139-4307

Received September 2, 2006

The iron(II) porphyrinogen dication, $[\mathrm{L^{\Delta\Delta}Fe^{II}}]^{2+}$, is a multielectron oxidant featuring the metal center in its reduced state and the ligand as the redox reservoir. Oxidations break the ligand's redox-active C–C bonds. Extremely short-lived excited states are consistent with extensive structural reorganization that accompanies charge-transfer excitation of the porphyrinogen.

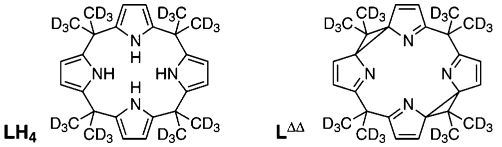

Figure 1. Porphyrinogen ligand used in this study, in its lowest (left) and highest (right) oxidation states.

The redox chemistry of coordination compounds is expanded when derived from a metal and a ligand working in concert. For such cases, redox activity is usually derived from (a) *one-electron* ligand-based redox couples and (b) the involvement of frontier orbitals of *mixed metal−ligand* character.[1−5] The porphyrinogen (Figure 1) actively participates in redox chemistry and does so in discrete *two-electron* steps by storing multielectron equivalents with the formation or breaking of one or two cyclopropane C−C bonds that are *localized* on the porphyrinogen ring.[6,7] Although transition-metal complexes of oxidized porphyrinogen have been structurally established for several metal−halo inorganic centers,[6−8] the general coordination and redox chemistry of such compounds have remained largely unexplored. We recently described an electron-transfer series for iron porphyrinogen,[7b]

$$[\mathrm{LFe^{II}}]^{2-} \xrightarrow{-e^-} [\mathrm{LFe^{III}}]^{-} \xrightarrow{-3e^-} [\mathrm{L^{\Delta\Delta}Fe^{II}}]^{2+} \qquad (1)$$

This Communication reports on the reactivity originating from the four-electron-oxidized iron porphyrinogen dication, $[\mathrm{L^{\Delta\Delta}Fe^{II}}]^{2+}$, and provides the first excited-state studies of porphyrinogen coordination compounds.

Unlike its reduced congeners $[\mathrm{LFe^{II}}]^{2-}$ and $[\mathrm{LFe^{III}}]^{-}$, $[\mathrm{L^{\Delta\Delta}Fe^{II}}]^{2+}$ reacts with anionic ligands. Exposure of $[\mathrm{L^{\Delta\Delta}Fe^{II}}](\mathrm{BF_4})_2$ to a stoichiometric or excess amount of $\mathrm{Bu_4NCl}$ in acetonitrile causes a shift in the ^{1}H β-pyrrole signals of $[\mathrm{L^{\Delta\Delta}Fe^{II}}]^{2+}$ from +59 and −7 ppm to +55 and −9 ppm, respectively (Figure S1). Alternatively, the same NMR signals are obtained upon three-electron oxidation of $\mathrm{Na[LFe^{III}]}$ with $\mathrm{AuCl_3}$, $\mathrm{KAuCl_4}$, or $\mathrm{PhICl_2}$. The simple shift of the ^{1}H β-pyrrole resonances shows that the symmetry of the macrocycle is maintained in the reaction and its oxidation state is not affected,[9] consistent with the axial coordination of $\mathrm{Cl^-}$ to Fe. Crystallographic analysis of the isolated material proves its identity to be $[\mathrm{L^{\Delta\Delta}Fe^{II}{-}Cl}](\mathrm{FeCl_4})$ (Figures 2 and S3). The UV−visible spectrum of the complex is independent of the synthetic path; the conspicuous bands of the $\mathrm{FeCl_4^-}$ counterion are observed at 313 and 363 nm.[10] The anion is produced by the presence of excess chloride, which causes extrusion of the Fe ion from a fraction of the metalloporphyrinogen units and limits the isolated yield to 56%. The powder Mössbauer spectrum of $[\mathrm{L^{\Delta\Delta}Fe^{II}{-}Cl}](\mathrm{FeCl_4})$ displays (in addition to the $\mathrm{FeCl_4^-}$ signal)[11] large quadrupole splitting and isomer shift, $\delta = 1.0$ mm/s, $\Delta E_q = 3.8$ mm/s, similar to those observed for $[\mathrm{L^{\Delta\Delta}Fe^{II}}](\mathrm{BF_4})_2$, corresponding to high-spin Fe(II).[7b]

The reactivity of $[\mathrm{L^{\Delta\Delta}Fe^{II}}]^{2+}$ switches from ligand substitution chemistry to redox chemistry upon reaction with

---

[*] To whom correspondence should be addressed. E-mail: nocera@mit.edu.

(1) Holm, R. H.; Balch, A. L.; Davison, A.; Maki, A. H.; Berry, T. E. *J. Am. Chem. Soc.* **1967**, *89*, 2866−2874 and references cited therein.

(2) Ray, K.; Bill, E.; Weyhermüller, T.; Wieghardt, K. *J. Am. Chem. Soc.* **2005**, *127*, 5641−5654 and references cited therein.

(3) Pierpont, C. G. *Coord. Chem. Rev.* **2001**, *216*, 99−125.

(4) Gutlich, P.; Dei, A. *Angew. Chem., Int. Ed.* **1997**, *36*, 2734−2736.

(5) (a) Blackmore, K. J.; Ziller, J. W.; Heyduk, A. F. *Inorg. Chem.* **2005**, *44*, 5559−5561. (b) Haneline, M. R.; Heyduk, A. F. *J. Am. Chem. Soc.* **2006**, *128*, 8410−8411.

(6) (a) Jubb, J.; Floriani, C.; Chiesi-Villa, A.; Rizzoli, C. *J. Am. Chem. Soc.* **1992**, *114*, 6571−6573. (b) De Angelis, S.; Solari, E.; Floriani, C.; Chiesi-Villa, A.; Rizzoli, C. *J. Am. Chem. Soc.* **1994**, *116*, 5691−5701. (c) De Angelis, S.; Solari, E.; Floriani, C.; Chiesi-Villa, A.; Rizzoli, C. *J. Am. Chem. Soc.* **1994**, *116*, 5712−5713. (d) Crescenzi, R.; Solari, E.; Floriani, C.; Chiesi-Villa, A.; Rizzoli, C. *J. Am. Chem. Soc.* **1999**, *121*, 1695−1706.

(7) (a) Bachmann, J.; Nocera, D. G. *J. Am. Chem. Soc.* **2004**, *126*, 2829−2837. (b) Bachmann, J.; Nocera, D. G. *J. Am. Chem. Soc.* **2005**, *127*, 4730−4743. (c) Bachmann, J.; Nocera, D. G. *Inorg. Chem.* **2005**, *44*, 6930−6932.

(8) Bhattacharya, D.; Dey, S.; Maji, S.; Pal, K.; Sarkar, S. *Inorg. Chem.* **2005**, *44*, 7699−7701.

(9) $\mathrm{L^{4-}}$ displays fourfold rotational symmetry in solution and in the solid state, $\mathrm{L^{\Delta\Delta}}$ twofold, and $\mathrm{L^{\Delta 2-}}$ none.

(10) Shapley, P. A.; Bigham, W. T.; Hay, M. T. *Inorg. Chim. Acta* **2003**, *345*, 255−260.

10.1021/ic0616636 CCC: $37.00

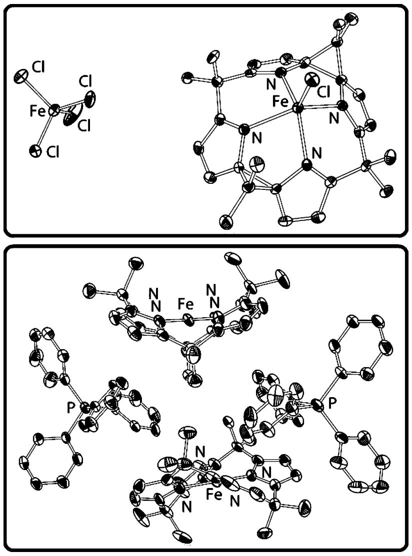

Figure 2. Crystal structures (thermal ellipsoids at 50% probability, H atoms and solvents omitted) of $[L^{\Delta\Delta}Fe^{II}Cl](FeCl_4)$ (top: orthorhombic, *Pbca*, R1 $[I > 2\sigma(I)] = 0.046$) and $(Ph_4P)[LFe^{III}]$ (bottom: monoclinic, $P2_1/c$, R1 $[I > 2\sigma(I)] = 0.059$). The asymmetric unit of the $[L^{\Delta\Delta}Fe^{II}Cl](FeCl_4)$ crystal contains two chemically identical ion pairs, only one of which is displayed. Full crystallographic data and color figures are available as Supporting Information.

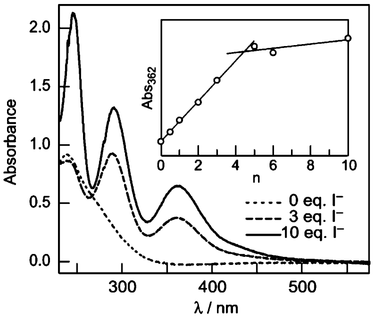

Figure 3. UV−visible spectra of $[L^{\Delta\Delta}Fe^{II}](BF_4)_2$ and Bu_4NI reaction mixtures of varying stoichiometries *n* (I^-:$[L^{\Delta\Delta}Fe^{II}]^{2+}$). The bands at 291 and 362 nm are due to I_3^- and those at 245 nm to I^-. Inset: 362-nm signal as a function of the stoichiometry, with linear fits intersecting at $n = 4.5$.

alcoholates such as $KOCMe_3$ or NaOMe. ^1H NMR reveals reduced $[LFe^{III}]^-$ (β-pyrrole peak at −72 ppm) as the only observable product. Reduction is prevented with the silanolate $NaOSiMe_3$; elemental analysis of the isolated material is consistent with the axially coordinated complex $[L^{\Delta\Delta}Fe^{II}{-}OSiMe_3](OSiMe_3)$. The $\delta = 0.4$ mm/s and $\Delta E_q = 1.0$ mm/s values from the Mössbauer spectrum are also consistent with the presence of a Fe(II) oxidation state. In solution, rotation around the Fe−O bond appears to be sterically hindered, as evidenced by four distinct ^1H NMR resonances for the β-pyrroles ($\delta = +107, +89, +84$, and $+27$ ppm; Figure S1). The silanolate, $[L^{\Delta\Delta}Fe^{II}{-}OSiMe_3]^+$, reacts with F^- in dichloromethane to yield a solid precipitate, which redissolves in acetonitrile. Its NMR spectrum shows the presence of a single paramagnetic product, with 2-fold symmetry (^1H β-pyrrole, +20 and +15 ppm; ^2H methyl, +7, +4, −4, and −21 ppm), and a large quadrupole splitting but a small isomer shift ($\delta = 0.3$ mm/s; $\Delta E_q = 3.2$ mm/s) is observed in the Mössbauer spectrum. The compound does not react with electron-rich substrates such as *cis*-cyclooctene, PPh_3, and $P(n\text{-}Bu)_3$. On the other hand, its reactions with $P(C_6F_5)_3$, tetracyanoethane, water, pyridinium chloride, and Ph_4PBr yield $[LFe^{III}]^-$ as the single paramagnetic product (see the crystal structure of $(Ph_4P)[LFe^{III}]$, Figures 2 and S4). This product likely results from single-electron redox reactions of the iron porphyrinogen species with substrate and solvent.

A well-defined chemistry of $[L^{\Delta\Delta}Fe^{II}]^{2+}$ is obtained with iodide as the reductant. On the basis of the previously determined redox potential of $[L^{\Delta\Delta}Fe^{II}]^{2+}$ (vs NHE), the thermodynamics of reaction (4) are favorable:[12]

$$I_3^- + 2e^- \rightarrow 3I^- \qquad E° = +0.53\ \text{V} \tag{2}$$

$$[L^{\Delta\Delta}Fe^{II}]^{2+} + 3e^- \rightarrow [LFe^{III}]^- \qquad E° = +0.77\ \text{V} \tag{3}$$

$$2[L^{\Delta\Delta}Fe^{II}]^{2+} + 9I^- \rightarrow 2[LFe^{III}]^- + 3I_3^- \qquad \Delta E \approx +0.24\ \text{V} \tag{4}$$

Upon mixing $[L^{\Delta\Delta}Fe^{II}](BF_4)_2$ with Bu_4NI, the characteristic UV−visible signature of triiodide immediately appears at 291 and 362 nm. The fate of the iron porphyrinogen byproduct was found to depend strongly on the experimental conditions. Under slow addition of a cold solution (−40 °C) of $[L^{\Delta\Delta}Fe^{II}](BF_4)_2$ to excess Bu_4NI (≥ 6 equiv), more than 80% of $[L^{\Delta\Delta}Fe^{II}]^{2+}$ is converted to $[LFe^{III}]^-$ according to eq 4. The remaining product is accounted for by LH_4, which presumably forms by $H^\bullet$ atom abstraction from the solvent. However, when a stoichiometric amount of I^- (4.5 equiv) is added to $[L^{\Delta\Delta}Fe^{II}]^{2+}$ at room temperature, all of the porphyrinogen is found as LH_4. The stoichiometry of the reaction was determined spectroscopically (Figure 3) to yield a $I^-/[L^{\Delta\Delta}Fe^{II}]^{2+}$ ratio of 9:2, as expected on the basis of eq 4. The reduction of $[L^{\Delta\Delta}Fe^{II}]^{2+}$ to $[LFe^{III}]^-$ by I^- is contrasted to the recently reported[8] oxidation of iron(III) tetrakis(*meso*-pentane-1,5-diylporphyrinogen), $[{}^*LFe^{III}]^-$, by excess I_2 to yield $[{}^*L^{\Delta\Delta}Fe^{II}{-}I](I_3){\cdot}I_2$. We note that the iodide complex was originally formulated[8] as $[{}^*L^{\Delta\Delta}Fe^{II}{-}I]^+(I_3)^-{\cdot}(I_2)^+(I_3)^-$. A review of the CIF file shows a miscount in the ions placed at special positions and indicates the correct formulation to be $[{}^*L^{\Delta\Delta}Fe^{II}{-}I](I_3){\cdot}I_2$.

The excited states of the iron porphyrinogens were examined by transient absorption spectroscopy. Density functional theory (DFT) calculations identify that the lowest-energy allowed transition of $[LFe^{III}]^-$ is derived from a one-electron ligand-to-metal charge transfer (LMCT) from the pyrroles to empty d(Fe) orbitals.[7b] Figure 4 displays the transient absorption spectrum of $[LFe^{III}]^-$. A prominent bleach of the ground-state absorption is superimposed on a broad positive transient signal. Beyond the initial spike attributed to pump−probe cross-correlation, the transient state relaxes back to the initial state monoexponentially with a $\tau = 13(\pm 3)$ ps lifetime at all wavelengths probed ($\lambda_{prb} = 500{-}806$ nm; Figure S3). Because the transient spectrum is more or less a bleach of the ground state, identifying the chemical nature of the excited state (e.g., a charge transfer $[L{\cdot}Fe^{II}]^-$[13] vs a vibrational excited state[14] of $[LFe^{III}]^-$) is difficult.

---

(11) Crystal packing forces seem to distort the anion slightly from its ideal tetrahedral symmetry: $\delta = 0.3$ mm/s; $\Delta E_q = 0.3$ mm/s.

(12) Atkins, P. W. *Physical Chemistry*, 6th ed.; Oxford University Press: Oxford, U.K., 1988; p 937.

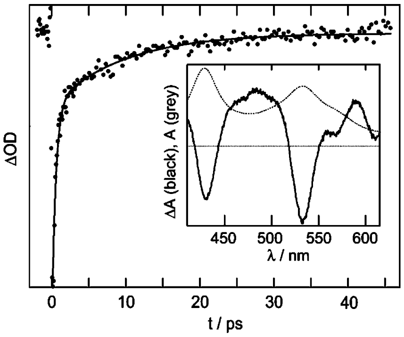

Figure 4. Transient absorption decay signal of Na[LFe^{III}] (black dots) probed at 530 nm upon excitation at 403 nm, with an exponential fit (gray line). Inset: transient spectrum at $t = 5$ ps (black) compared to the ground-state absorption (dotted gray trace); the horizontal line defines the zero.

Fast excited-state dynamics are also observed for [$L^{\Delta\Delta}Fe^{II}Cl$]$^+$. The lowest unoccupied molecular orbitals of [$L^{\Delta\Delta}Fe^{II}Cl$]$^+$ are ligand-based, and the highest occupied molecular orbitals correspond to the nonbonding electron of the chloride ligand, with metal-centered singly occupied molecular orbitals at intermediate energies (Figure S2), suggesting the presence of a chloride-to-porphyrinogen charge-transfer contribution. A weak positive signal at 806 nm appears promptly after 550-nm excitation and subsequently decays monoexponentially with a lifetime of $\tau = 30(\pm 10)$ ps. This transient state does not support excited-state bimolecular reactivity. Indeed, no photoreaction is observed upon steady irradiation into the absorption manifold of [$L^{\Delta\Delta}Fe^{II}Cl$]$^+$, even in the presence of $H^\bullet$ atom donors such as terpinene. We note that a photoreaction is observed when the absorption envelope of the $FeCl_4^-$ counterion is excited (350 nm $< \lambda <$ 450 nm). $H^\bullet$ atom abstraction from terpinene by [$FeCl_4^-$]* leads to its quantitative aromatization to cymene.

Nonradiative decay of iron porphyrinogens occurs before the geometric reorganization and bonding changes attendant to the two-electron transformations of the ligand can occur. This observation contrasts the photochemistry of iron porphyrins. Chloroiron(III) porphyrins, $PFe^{III}-Cl$, undergo facile metal−ligand bond homolysis to $PFe^{II} + Cl^\bullet$ upon chloride-to-iron(III) LMCT excitation,[15] despite the short excited-state lifetime (shorter than that reported here for [$L^{\Delta\Delta}Fe^{II}Cl$]$^+$). In the case of the porphyrins, excitation is localized in the Cl−Fe bond that is being activated. Therefore, the structural rearrangement caused by the excited state directly activates the chemically relevant vibrational mode. Consistent with this interpretation, $\pi \rightarrow \pi^*$ excitation of the porphyrin ring of $PFe^{III}-Cl$ does not result in an efficient photochemistry. In the case of the porphyrinogens, the excitation occurs between bonds that are weakly coupled, i.e., the Fe−Cl bond and the $C^\alpha-C^\alpha$ bonds of the porphyrinogen ring. We expect that this phototransformation is highly nonadiabatic, thus accounting for the lack of porphyrinogen photochemistry.

The reaction chemistry of [$L^{\Delta\Delta}Fe^{II}$]$^{2+}$ is summarized in Figure 5. The neutral charge of the oxidized $L^{\Delta\Delta}$ macrocycle makes the cationic iron center prone to axial coordination. [$L^{\Delta\Delta}Fe^{II}$]$^{2+}$ undergoes facile multielectron reduction to [LFe^{III}]$^-$ by iodide and alcoholates. In such transformations, the two-electron $C^\alpha-C^\alpha$ bonds of the ligand function as the multielectron reservoir, allowing the oxidation state of the metal to be minimally affected. The porphyrinogen is unusual compared to typical coordination compounds in that the highly oxidizing center is located on the ligand and not the metal. Thus, the metal remains a poor Lewis acid even when the compound is highly oxidized. Other consequences of ligand-based redox equivalency are evident in the photophysics of these compounds. The excited states of oxidized chloroiron complexes of porphyrins and porphyrinogen exhibit widely different reactivities despite similar lifetimes. In the latter case, charge-transfer photoexcitation is followed by fast back-transfer. The extensive structural reorganization of the ligand and bond-breaking/-making within it that accompany redox events such as that potentially derived from charge-transfer excitation appear to be sufficiently demanding that they cannot compete with vibrational relaxation of the electronic excited state.[16] Consequently, the compound is photostable.

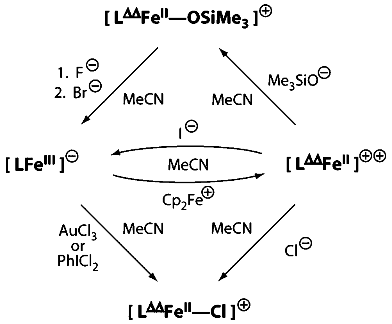

Figure 5. Reactivity originating from oxidized iron porphyrinogen.

Acknowledgment. This work was supported under a grant from the National Science Foundation (Grant CHE-0132680) and made use of the Shared Experimental Facilities at MIT's CMSE, a MRSEC Program of the National Science Foundation (Grant DMR 02-13282).

Supporting Information Available: Experimental procedures, NMR spectra, DFT results, ultrafast spectroscopy data, and tables of crystallographic data. This material is available free of charge via the Internet at http://pubs.acs.org.

IC0616636

---

(13) The spectra of [LFe^{II}]$^{2-}$ and aromatic cation radical of L show no structured absorption in the visible region (see ref 7b).

(14) Bilsel, O.; Milam, S. N.; Girolami, G. S.; Suslick, K. S.; Holten, D. *J. Phys. Chem.* **1993**, *97*, 7216−7221.

(15) (a) Hendrickson, D. N.; Kinnaird, M. G.; Suslick, K. S. *J. Am. Chem. Soc.* **1987**, *109*, 1243−1244. (b) Suslick, K. S.; Watson, R. A. *Inorg. Chem.* **1991**, *30*, 912−919. (c) Suslick, K. S.; Watson, R. A. *New J. Chem.* **1992**, *16*, 633−642.

(16) Because the porphyrinogen ligand is redox-active, charge-transfer excited states can, in general, be described in a first approximation as transient states in which electron transfer has occurred between two parts of the species, one of which is the macrocycle in the case of iron porphyrinogens. Electron transfer to and from the porphyrinogen ligand is accompanied by bond-breaking/-making events, and therefore charge-transfer excitation in iron porphyrinogens is coupled to structural reorganization. Such coupling between nuclear and electronic coordinates would facilitate efficient nonradiative relaxation, thus circumventing possible further chemically relevant transformations.